

**Electronic Supplementary Information**

**Rhenium(V)-oxo corrolazines: isolating redox-active ligand reactivity**

*Jan Paulo T. Zaragoza, Maxime A. Siegler, and David P. Goldberg\**

\*E-mail: dpg@jhu.edu

Department of Chemistry, The Johns Hopkins University, 3400 N. Charles Street, Baltimore, MD 21218, USA

**Materials.** The metal-free ligand octakis(*p*-*tert*-butylphenyl)corrolazine ( $\text{TBp}_8\text{CzH}_3$ , **1**) was synthesized and purified according to a previously published procedure.<sup>1</sup> The oxonium acid  $[\text{H}(\text{OEt}_2)_2][\text{B}(\text{C}_6\text{F}_5)_4]$  ( $\text{HBArF}$ ), was prepared according to the improved one-pot synthesis reported by Kühn.<sup>2</sup> Dichloromethane, toluene and acetonitrile were purified via a Pure-Solv solvent purification system from Innovative Technologies, Inc. Tetrabutylammonium hexafluorophosphate ( $\text{TBAPF}_6$ ) and 9,10-dihydroanthracene (DHA) were recrystallized twice in ethanol and dried under vacuum prior to use. Deuterated solvents for NMR measurements and  $\text{H}_2^{18}\text{O}$  (97%) were obtained from Cambridge Isotopes, Inc. All other reagents were purchased from Sigma-Aldrich at the highest level of purity and used as received.

**Instrumentation.** UV-vis spectra were collected using a Varian Cary 50 Bio spectrophotometer or a Hewlett-Packard Agilent 8453 diode-array spectrophotometer with a 3.5 mL air-free quartz cuvette (path length = 1 cm) fitted with a septum. LDI-MS was conducted on a Bruker Autoflex III TOF/TOF instrument equipped with a nitrogen laser at 335 nm using an MTP 384 ground steel target plate.  $^1\text{H}$  NMR spectra were recorded on a Bruker Avance 400 or 300 MHz NMR spectrometer at 298 or 213 K.  $^{13}\text{C}$  NMR spectrum were recorded on a Bruker Avance 600 MHz NMR spectrometer at 298 K under an operating frequency of 151 MHz. Elemental analysis was performed at Atlantic Microlab, Inc., Norcross, GA. Gas chromatography (GC) was carried out on an Agilent 6850 gas chromatograph fitted with a DB-5 5% phenylmethyl siloxane capillary column (30 m x 0.32 mm x 0.25  $\mu\text{m}$ ) and equipped with a flame-ionization detector. Signals were quantified using an eicosane internal standard. Cyclic voltammetry was performed on an EG&G Princeton Applied Research potentiostat/galvanostat model 263A with a three-electrode system consisting of a glassy carbon working electrode, a  $\text{Ag}/\text{AgNO}_3$  non-aqueous reference electrode (0.01 M  $\text{AgNO}_3$  with 0.1 M  $\text{TBAPF}_6$  in  $\text{CH}_3\text{CN}$ ), and a platinum wire counter electrode. Measurements were performed with 0.10 M  $\text{TBAPF}_6$  as the supporting electrolyte in dry  $\text{CH}_2\text{Cl}_2$  at ambient temperatures under an atmosphere of  $\text{N}_2$ . Potentials were calculated from  $E_{1/2} = (E_{pa} + E_{pc})/2$  with a ferrocenium/ferrocene ( $\text{Fc}^+/\text{Fc}$ ) external reference and converted to SCE.<sup>3</sup> Electron paramagnetic resonance (EPR) spectra were recorded with a Bruker EMX spectrometer equipped with a Bruker ER 041 X G microwave bridge and a continuous-flow liquid helium cryostat (ESR900) coupled to an Oxford Instruments TC503 temperature controller for low temperature data collection. EPR signals were quantified by double integration and comparison with a standard  $[\text{Ar}'_3\text{N}]^{+}[\text{SbCl}_6]^{-}$  ( $\text{Ar}' = 4$ -bromophenyl) calibration curve. IR spectra were collected from a Thermo Scientific Nicolet iS5 FT-IR Spectrometer equipped with an iD5 Diamond ATR.

**Synthesis of  $\text{Re}^{\text{V}}(\text{O})(\text{TBp}_8\text{Cz})$  (**2**).** To a solution of  $\text{TBp}_8\text{CzH}_3$  (**1**) (37 mg, 0.028 mmol) in decalin (20 mL) was added  $\text{ReCl}_5$  (100 mg, 0.275 mmol) and refluxed under Ar for 2 h. The reaction mixture was opened to air and cooled down to 25 °C. The solvent was removed by vacuum distillation, and purification by column chromatography on silica gel (40:60  $\text{CH}_2\text{Cl}_2$ /hexanes,  $R_f = 0.86$ ) afforded a green solid (43 mg, 99 % yield). Vapor diffusion of acetonitrile into a concentrated toluene solution of **2** gave single crystals (dark blue blocks) suitable for X-ray structure determination. UV-Vis ( $\text{CH}_2\text{Cl}_2$ ):  $\lambda_{\text{max}}$ , nm ( $\epsilon \times 10^{-4} \text{ M}^{-1} \text{ cm}^{-1}$ ): 460 (9.33), 670 (4.67).  $^1\text{H}$  NMR (400 MHz,  $\text{CD}_2\text{Cl}_2$ )  $\delta$  (ppm) 8.44 (d,  $J = 7.6$  Hz, 8H), 8.03 (d,  $J = 8.2$  Hz, 4H), 7.74 (d,  $J = 8.1$  Hz, 8H), 7.55 (dd,  $J = 7.6$  Hz, 8H), 7.26 (d,  $J = 8.2$  Hz, 4H), 1.54 (d,  $J = 5.5$  Hz, 36H), 1.45 (s, 18H), 1.41 (s, 18H).  $^{13}\text{C}\{\text{H}\}$  NMR (151 MHz,  $\text{CD}_2\text{Cl}_2$ )  $\delta$  (ppm) 152.58, 152.41, 152.33, 149.67, 145.21, 144.31, 143.94, 142.09, 138.98, 138.80, 137.94, 133.99, 133.87, 133.80, 133.04, 132.56, 132.38, 132.25, 126.76, 126.68, 126.37, 126.26, two aromatic carbon resonances not resolved, 36.17 ( $\underline{\text{C}}(\text{CH}_3)_3$ ), 36.00 ( $\underline{\text{C}}(\text{CH}_3)_3$ ), 33.34 ( $\underline{\text{C}}(\text{CH}_3)_3$ ), one  $\underline{\text{C}}(\text{CH}_3)_3$  not resolved, 32.69 ( $\underline{\text{CH}_3}$ ), 32.57 ( $\underline{\text{CH}_3}$ ), 31.10 ( $\underline{\text{CH}_3}$ ), 30.77 ( $\underline{\text{CH}_3}$ ). FT-IR ( $\text{cm}^{-1}$ , ATR) 2956, 1471, 1362, 1265, 1102, 997 ( $\text{Re}-^{16}\text{O}$ ), 830, 743, 561. LDI-MS (m/z): isotopic cluster centered at 1557.38 ( $\text{M}^+$ ). Anal. Calcd for  $\text{C}_{96}\text{H}_{104}\text{N}_7\text{ORe}$ : C, 74.00; H, 6.73; N, 6.29. Found: C, 73.92; H, 6.69; N, 6.29. CV ( $\text{CH}_2\text{Cl}_2$ ),  $E_{1/2} = 1.04$  V vs SCE ( $\text{Cz}^+/\text{Cz}$ ).

**$^{18}\text{O}$  incorporation studies.**  $\text{Re}^{\text{V}}(^{18}\text{O})(\text{TBp}_8\text{Cz})$  (**2- $^{18}\text{O}$** ) was synthesized in a similar manner as described above, with slight modifications as follows: A solution of  $\text{TBp}_8\text{CzH}_3$  (**1**) (23 mg, 0.017 mmol) and  $\text{H}_2^{18}\text{O}$  (25  $\mu\text{L}$ , 1.4 mmol) was allowed to equilibrate for 30 min in decalin (10 mL) at room temperature in an Ar atmosphere. To this solution was added  $\text{ReCl}_5$  (160 mg, 0.51 mmol), and the reaction was refluxed for 1 h.

The solvent was removed, and the product was purified as described for **2**. (19 mg, 71 % yield). LDI-MS (m/z): isotopic cluster centered at 1560.28 ( $M^+$ ). FT-IR ( $\text{cm}^{-1}$ , ATR) 2956, 1471, 1362, 1265, 1102, 945 (Re- $^{18}\text{O}$ ), 830, 743, 561.

**Synthesis of  $[\text{Re}^{\text{V}}(\text{O})(\text{TBP}_8\text{Cz})(\text{H})]^+[\text{BArF}]^-$  (3(BArF))**. To a solution of the  $\text{Re}^{\text{V}}(\text{O})$  complex **2** (15 mg, 9.6  $\mu\text{mol}$ ) in 750  $\mu\text{L}$   $\text{CH}_2\text{Cl}_2$  was added 1 equiv of HBArF. A color change from green to brown was observed. This solution was evaporated to dryness and the solid was used for further characterization. UV-Vis ( $\text{CH}_2\text{Cl}_2$ ):  $\lambda_{\text{max}}$ , nm ( $\epsilon \times 10^4 \text{ M}^{-1} \text{ cm}^{-1}$ ): 470 (6.65), 723 (4.19).  $^1\text{H}$  NMR (400 MHz,  $\text{CD}_2\text{Cl}_2$ )  $\delta$  (ppm) 13.49 (s, 1H), 8.50 (m, 2H), 8.41 (m, 3H), 8.04 (m, 5H), 7.94 (m, 2H), 7.82 – 7.73 (m, 8H), 7.63 – 7.52 (m, 8H), 7.34 – 7.27 (m, 4H), 1.57 (m, 36H), 1.49 (s, 18H), 1.41 (m, 18H). FT-IR ( $\text{cm}^{-1}$ , ATR) 3280 (N-H), 2963, 1644\*, 1513\*, 1461\*, 1272\*, 1108, 1083\*, 1002, 975\*, 833, 775\*, 768\*, 754\*, 725\*, 683\*, 660\*, 609\* (\* = peaks from BArF). LDI-MS (m/z): isotopic cluster centered at 1558.45 ( $M^+$ ). Anal. Calcd for  $\text{C}_{120}\text{H}_{106}\text{BF}_{19}\text{N}_7\text{ORe C}$ , 64.92; H, 4.81; N, 4.42. Found: C, 65.16; H, 4.75; N, 4.48. CV ( $\text{CH}_2\text{Cl}_2$ ),  $E_{\text{pc}} = -0.17$  vs SCE.

**Generation of  $[\text{Re}^{\text{V}}(\text{O})(\text{TBP}_8\text{Cz})]^+[\text{X}^-]$  (4(X)) (X =  $\text{SbCl}_6^-$ ,  $\text{NO}_3^-$ )**. To a solution of **2** (12  $\mu\text{M}$ , 2 mL) in  $\text{CH}_2\text{Cl}_2$  was added  $[\text{Ar}_3\text{N}]^+[\text{SbCl}_6]^-$  (1 equiv, 20  $\mu\text{L}$  in  $\text{CH}_2\text{Cl}_2$ ) or cerium(IV) ammonium nitrate (CAN) (1 equiv, 20  $\mu\text{L}$  in  $\text{CH}_3\text{CN}$ ) in  $\text{CH}_2\text{Cl}_2$ . A color change from green to brown was noted. UV-Vis ( $\text{CH}_2\text{Cl}_2$ ): **4(SbCl<sub>6</sub><sup>-</sup>)**,  $\lambda_{\text{max}}$ , nm ( $\epsilon \times 10^4 \text{ M}^{-1} \text{ cm}^{-1}$ ): 445 (4.53), 760 (1.66). **4(NO<sub>3</sub><sup>-</sup>)**,  $\lambda_{\text{max}}$ , nm ( $\epsilon \times 10^4 \text{ M}^{-1} \text{ cm}^{-1}$ ): 445 (4.04), 760 (1.66), 850 (0.59). EPR (298 K) g = 2.00, linewidth = 10 G; (16 K) g = 2.00, linewidth = 18 G;

**Single Crystal X-ray Crystallography.** All reflection intensities were measured at 110(2) K using a SuperNova diffractometer (equipped with Atlas detector) with Cu  $K\alpha$  radiation ( $\lambda = 1.54178 \text{ \AA}$ ) under the program CrysAlisPro (Version 1.171.36.32 Agilent Technologies, 2013). The same program was used to refine the cell dimensions and for data reduction. The structure was solved with the program SHELXS-2013<sup>4</sup> and was refined on  $F^2$  with SHELXL-2013.<sup>4</sup> Analytical numeric absorption corrections based on a multifaceted crystal model were applied using CrysAlisPro. The temperature of the data collection was controlled using the system Cryojet (manufactured by Oxford Instruments). The H atoms were placed at calculated positions using the instructions AFIX 43 or AFIX 137 with isotropic displacement parameters having values 1.2 or 1.5 times  $U_{\text{eq}}$  of the attached C atoms.

The structure for  $\text{Re}^{\text{V}}(\text{O})(\text{TBP}_8\text{Cz})$  is entirely disordered over two orientations, and the occupancy factor of the major component of the disorder refines to 0.709(2). The structure also contains some partially occupied and disordered solvent molecules (toluene and acetonitrile). The contribution of those solvent molecules has been taken out in the final refinement (SQUEEZE<sup>5</sup> details are provided in the CIF file), which also allows to keep the data-to-parameter ratio to an acceptable level.

Data for  $\text{Re}^{\text{V}}(\text{O})(\text{TBP}_8\text{Cz})$  (**2**): Fw = 1558.06, dark blue-black block,  $0.32 \times 0.23 \times 0.18 \text{ mm}^3$ , triclinic, *P*-1 (no. 2),  $a = 15.7923(2)$ ,  $b = 16.6247(3)$ ,  $c = 21.4456(3) \text{ \AA}$ ,  $\alpha = 70.8548(14)$ ,  $\beta = 70.4554(13)$ ,  $\gamma = 71.4233(13)^\circ$ ,  $V = 4872.60(14) \text{ \AA}^3$ ,  $Z = 2$ ,  $D_x = 1.062 \text{ g cm}^{-3}$ ,  $\mu = 2.767 \text{ mm}^{-1}$ ,  $T_{\min}-T_{\max}$ : 0.542–0.723. 63946 Reflections were measured up to a resolution of  $(\sin \theta/\lambda)_{\text{max}} = 0.62 \text{ \AA}^{-1}$ . 18949 Reflections were unique ( $R_{\text{int}} = 0.0204$ ), of which 17574 were observed [ $I > 2\sigma(I)$ ]. 1929 Parameters were refined using 3989 restraints.  $R1/wR2$  [ $I > 2\sigma(I)$ ]: 0.0539/0.1500.  $R1/wR2$  [all refl.]: 0.0578/0.1546.  $S = 1.099$ . Residual electron density found between −0.98 and 1.77 e  $\text{\AA}^{-3}$ .

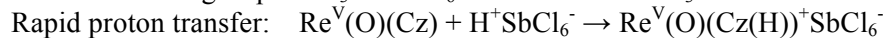
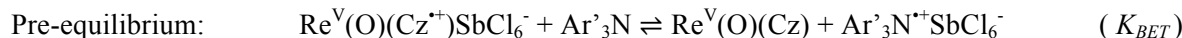
**Computational Methods.** Computational studies on the rhenium complexes  $^1[\text{Re}^{\text{V}}(\text{O})(\text{H}_8\text{Cz})]$ ,  $^1[\text{Re}^{\text{V}}(\text{OH})(\text{H}_8\text{Cz})]^+$  and  $^1[\text{Re}^{\text{V}}(\text{O})(\text{H}_8\text{Cz}(\text{H}))]^+$  were performed using the *Orca* program package.<sup>6</sup> Geometry optimizations and frequency calculations were performed using hybrid density functional theory PBE0<sup>7</sup> with the LANL2TZ<sup>8</sup> basis set on Re and the 6-31G\*\*<sup>9</sup> basis set on the remaining atoms, as suggested by Deakyne, and co-workers<sup>10</sup> for monooxorhenium(V) complexes. The initial geometry of the rhenium-oxo corrolazine  $^1[\text{Re}^{\text{V}}(\text{O})(\text{H}_8\text{Cz})]$  was obtained from the  $\text{Re}^{\text{V}}(\text{O})(\text{TBP}_8\text{Cz})$  X-ray crystal structure with all the *p*-tert-butylphenyl groups replaced with hydrogens. Subsequent calculations on the protonated complexes

$^1[\text{Re}^{\text{V}}(\text{OH})(\text{H}_8\text{Cz})]^+$  or  $^1[\text{Re}^{\text{V}}(\text{O})(\text{H}_8\text{Cz(H)})]^+$  were achieved by manually adding a proton on either the oxo ligand or the *meso*-N position of the corrolazine ligand, then allowing the structures to optimize without constraints. Optimized geometries were used for frequency calculations at the same level of theory to ensure the local minimum nature of the geometry (without any imaginary frequencies).

**UV-vis Kinetics Studies** The  $\text{Re}^{\text{V}}(\text{O})$  complex **4** was generated *in situ* by addition of 1 equiv of  $[\text{Ar}'_3\text{N}]^{+\cdot}[\text{SbCl}_6]^-$  (in  $\text{CH}_2\text{Cl}_2$ ) or CAN (in  $\text{CH}_3\text{CN}$ ) to an amount of  $\text{Re}^{\text{V}}(\text{O})(\text{TBP}_8\text{Cz})$  (**2**) ( $12 \mu\text{M}$ ,  $\text{CH}_2\text{Cl}_2$ ). Upon complete formation of **4**, varying amounts of DHA ( $60 - 450 \text{ mM}$ ) were added to start the reaction. The spectral change showed isosbestic conversion of **4** ( $\lambda_{\text{max}} = 460, 760 \text{ nm}$ ) to **3** ( $\lambda_{\text{max}} = 470, 723 \text{ nm}$ ), or **2** ( $\lambda_{\text{max}} = 460, 670 \text{ nm}$ ), in the presence of  $\text{NO}_3^-$  ions. The pseudo-first-order rate constants,  $k_{\text{obs}}$ , for these reactions were obtained by non-linear least-squares fitting of the plots of absorbance at  $670 \text{ nm}$  ( $\text{Abs}_t$ ) versus time ( $t$ ) according to the equation  $\text{Abs}_t = \text{Abs}_0 + (\text{Abs}_0 - \text{Abs}_f) \exp(-k_{\text{obs}}t)$  where  $\text{Abs}_0$  and  $\text{Abs}_f$  are initial and final absorbance, respectively. Second order rate constants ( $k$ ) were obtained from the slope of the best-fit line from a plot of  $k_{\text{obs}}$  vs substrate concentration.

**Product Analysis.** The complex  $\text{Re}^{\text{V}}(\text{O})(\text{TBP}_8\text{Cz})$  (**2**) ( $2 \text{ mM}$  in  $2 \text{ mL}$  of  $\text{CH}_2\text{Cl}_2$ ) was combined with a solution of  $[\text{Ar}'_3\text{N}]^{+\cdot}[\text{SbCl}_6]^-$  (1 equiv in  $\text{CH}_2\text{Cl}_2$ ) to form  $\text{Re}^{\text{V}}(\text{O})(\text{TBP}_8\text{Cz}^{+\cdot})$  (**4**). An amount of 9,10-dihydroanthracene (5 equiv) was then added and the reaction was monitored by UV-vis spectroscopy, which showed complete conversion to **3**. The solution was directly injected onto the GC. Yields were calculated from a calibration curve with eicosane as an internal standard.

### Proposed mechanism for the reaction of **4**( $\text{SbCl}_6^-$ ) with DHA.



Thus, the rate law can be formulated as:

$$\text{rate} = k_I [(\text{Ar}'_3\text{N})^{+\cdot}(\text{SbCl}_6)] [\text{DHA}]$$

From the rate law, the reaction is zero-order in  $\text{Re}^{\text{V}}(\text{O})(\text{Cz}^{+\cdot})\text{SbCl}_6^-$ , and first order in both  $\text{Ar}'_3\text{N}^{+\cdot}\text{SbCl}_6^-$  and 9,10-DHA.

### References

1. B. Ramdhanie, C. L. Stern and D. P. Goldberg, *J. Am. Chem. Soc.*, 2001, **123**, 9447-9448.
2. S. F. Rach, E. Herdtweck and F. E. Kühn, *J. Organomet. Chem.*, 2011, **696**, 1817-1823.
3. N. G. Connelly and W. E. Geiger, *Chem. Rev.*, 1996, **96**, 877-910.
4. G. M. Sheldrick, *Acta Crystallogr., Sect. A: Found. Crystallogr.*, 2008, **64**, 112-122.
5. A. L. Spek, *J. Appl. Crystallogr.*, 2003, **36**, 7-13.
6. F. Neese, *WIREs: Comput. Mol. Sci.*, 2012, **2**, 73-78.
7. (a) C. Adamo and V. Barone, *J. Chem. Phys.*, 1999, **110**, 6158-6170; (b) M. Ernzerhof and G. E. Scuseria, *J. Chem. Phys.*, 1999, **110**, 5029-5036.
8. L. E. Roy, P. J. Hay and R. L. Martin, *J. Chem. Theory Comput.*, 2008, **4**, 1029-1031.
9. (a) P. C. Hariharan and J. A. Pople, *Theoret. Chim. Acta*, 1973, **28**, 213-222; (b) M. M. Franci, W. J. Pietro, W. J. Hehre, J. S. Binkley, M. S. Gordon, D. J. DeFrees and J. A. Pople, *J. Chem. Phys.*, 1982, **77**, 3654-3665.
10. D. W. Demoin, Y. Li, S. S. Jurisson and C. A. Deakyne, *Comp. Theor. Chem.*, 2012, **997**, 34-41.

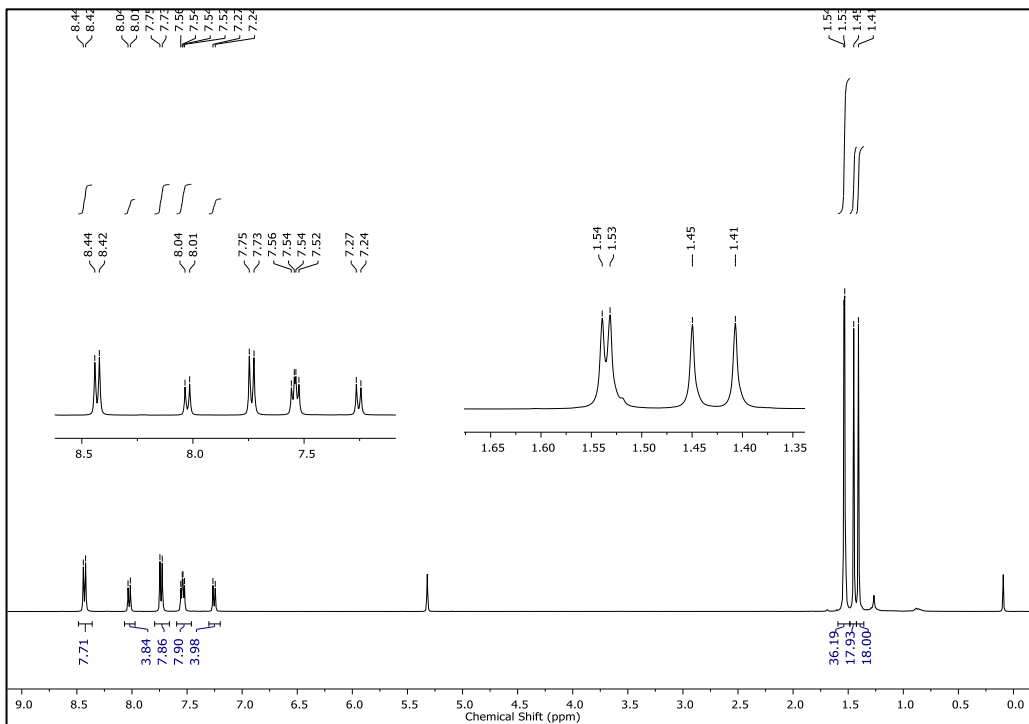


**Fig. S1.**  $^1\text{H}$  NMR spectrum (400 MHz) of  $\text{Re}^{\text{V}}(\text{O})(\text{TBP}_8\text{Cz})$  (**2**) in  $\text{CD}_2\text{Cl}_2$ .

**Table S1.** Selected Bond distances (Å) and angles (°) for Re<sup>V</sup>O(TBP<sub>8</sub>Cz) (2).

Re1 – N1	1.960(5)
Re1 – N2	1.948(5)
Re1 – N4	2.013(4)
Re1 – N6	1.986(6)
Re1 – (N <sub>pyrrole</sub> ) <sub>plane</sub>	0.74
Re1 – (23-atom) <sub>core</sub>	1.00
C <sub>β</sub> – C <sub>β</sub> (av)	1.395(19)
C <sub>α</sub> – C <sub>β</sub> (av)	1.436(26)
C <sub>α</sub> – C <sub>α</sub> (C4-C5)	1.522(9)
C <sub>α</sub> – N <sub>pyrrole</sub> (av)	1.381(24)
C <sub>α</sub> – N <sub>meso</sub> (av)	1.324(22)
Re1 – O1	1.682(9)
N1 – Re1 – N2	76.8(4)
N2 – Re 1 – N4	84.6(3)
N4 – Re 1 – N6	84.7(3)
N6 – Re 1 – N1	81.8(4)
N1 – Re 1 – O1	113.3(3)
N2 – Re 1 – O1	113.9(5)
N4 – Re 1 – O1	110.9(3)
N6 – Re 1 – O1	110.0(5)

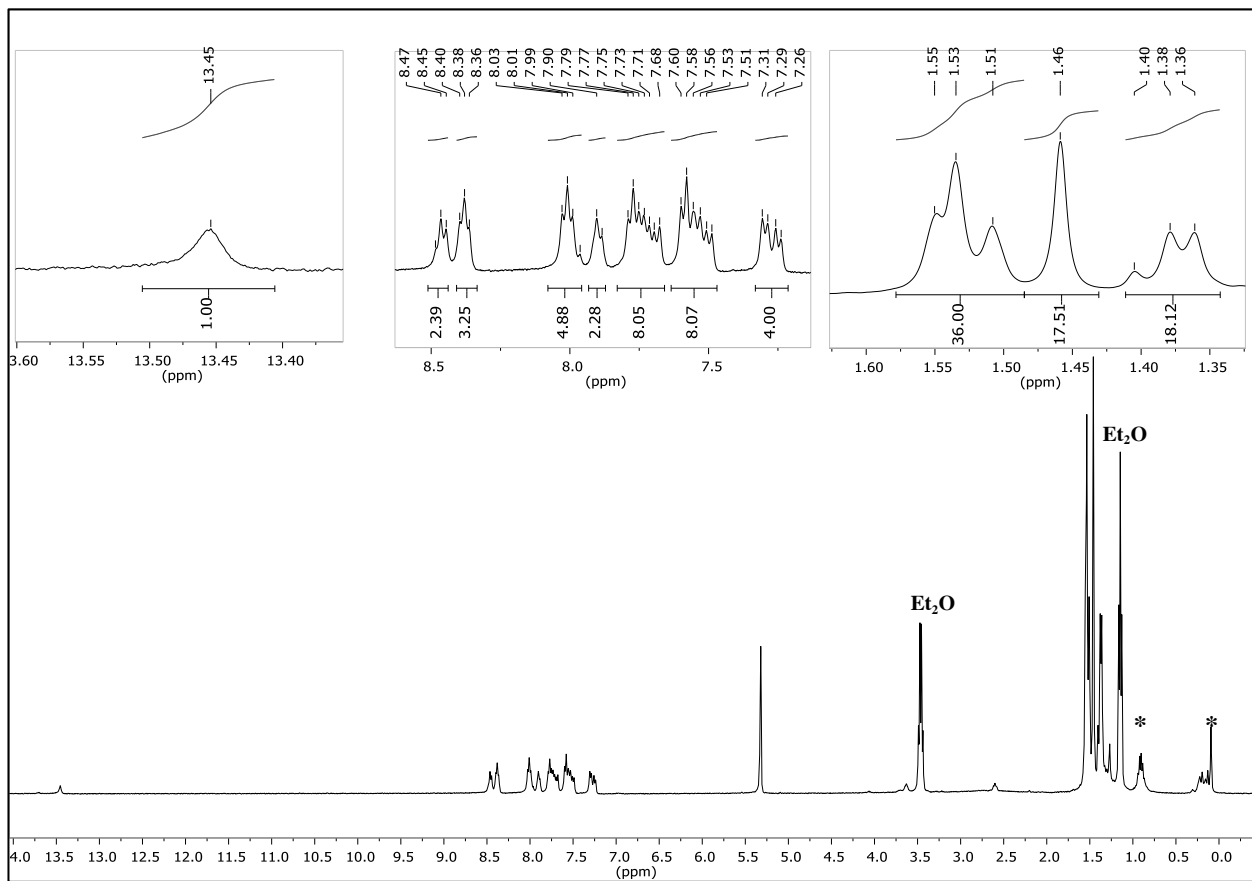


**Fig. S2.**  $^1\text{H}$  NMR spectrum (400 MHz) of  $\text{Re}^{\text{V}}(\text{O})(\text{TBP}_8\text{CzH})^+[\text{BArF}]^-$  (**3**) $(\text{BArF}^-)$  in  $\text{CD}_2\text{Cl}_2$ . \* = solvent impurities.

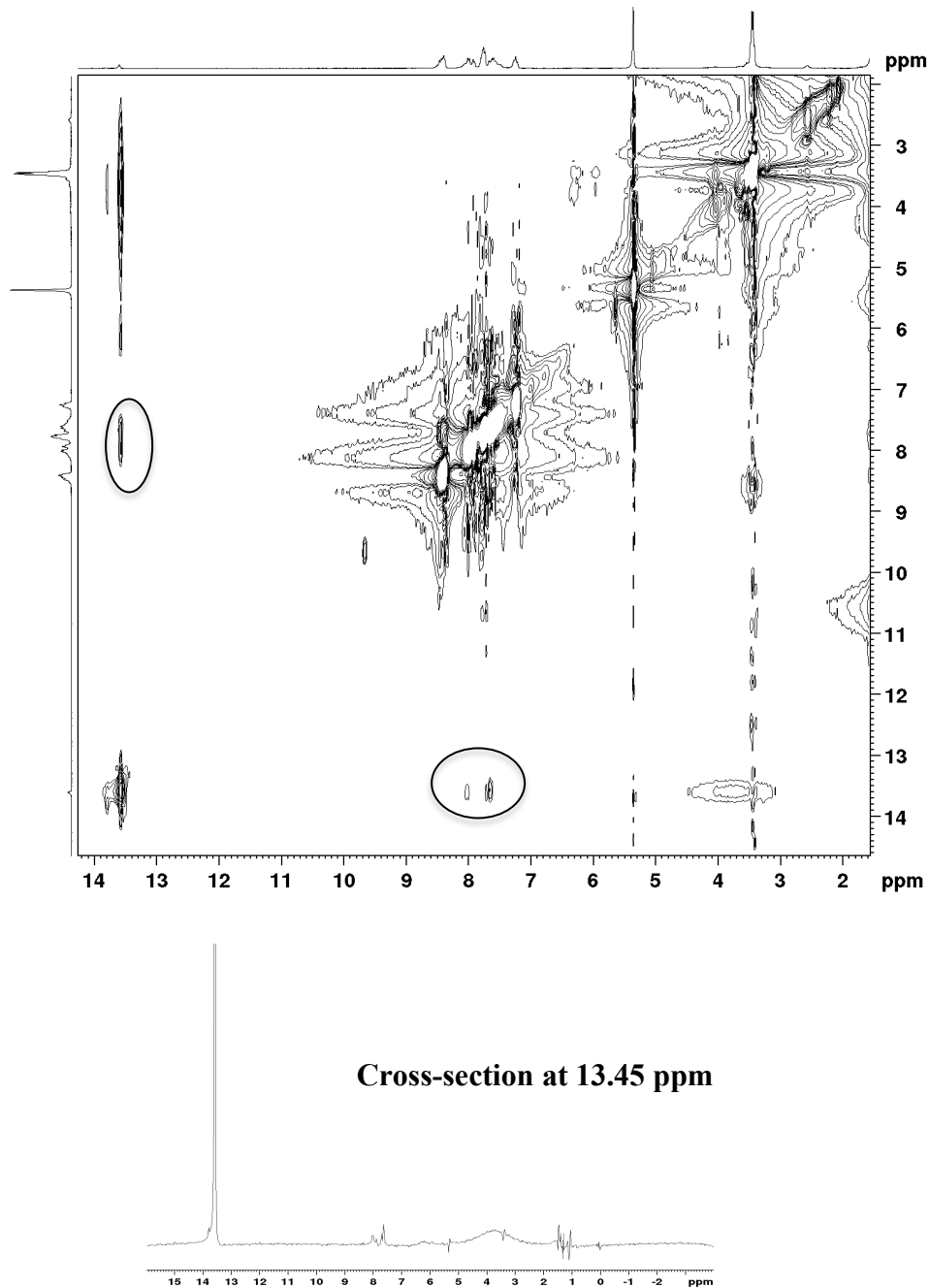


**Fig. S3.**  $^1\text{H}$ - $^1\text{H}$  2D NOESY (300 MHz) of  $\text{Re}^{\text{V}}(\text{O})(\text{TBP}_8\text{CzH})^+[\text{BArF}]^-$  (**3**)( $\text{BArF}^-$ ) in  $\text{CD}_2\text{Cl}_2$  at 213 K. Relevant through-space interactions of the N-H peak at 13.45 ppm with the aryl protons at 7.7 and 8 ppm are encircled. Cross-section at 13.45 ppm displayed on the bottom.

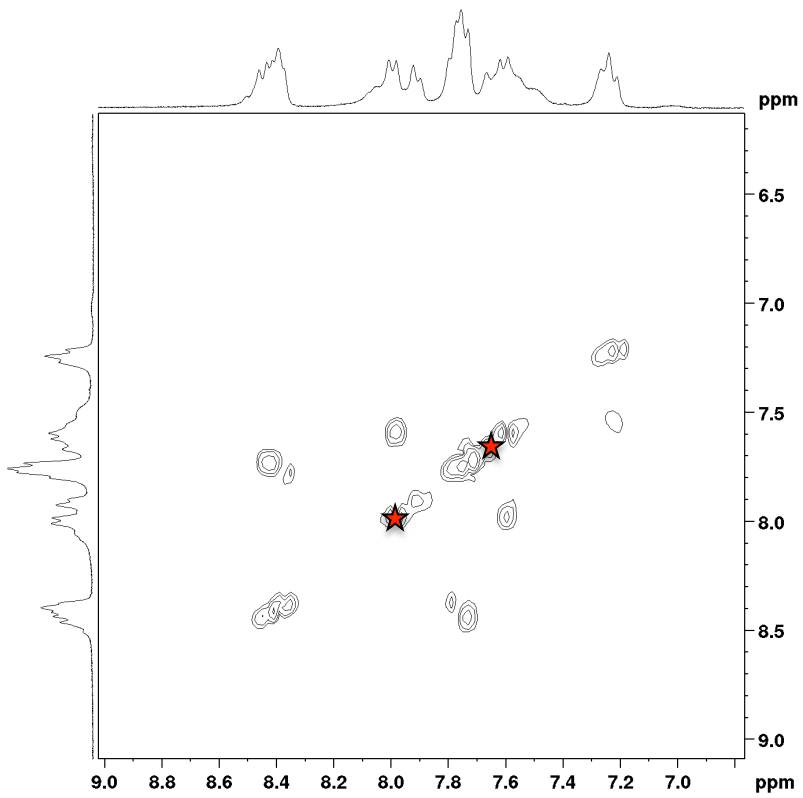


**Fig. S4.**  $^1\text{H}$ - $^1\text{H}$  2D COSY (300 MHz) of  $\text{Re}^{\text{V}}(\text{O})(\text{TBP}_8\text{CzH})^+[\text{BArF}]^-$  (**3**)( $\text{BArF}^-$ ) (aromatic region) in  $\text{CD}_2\text{Cl}_2$  at 213 K. The aryl protons at 7.7 and 8.0 ppm (red stars) are highlighted, showing no correlation between them. These data show that the two aryl C-H resonances arise from protons on separate benzene rings.

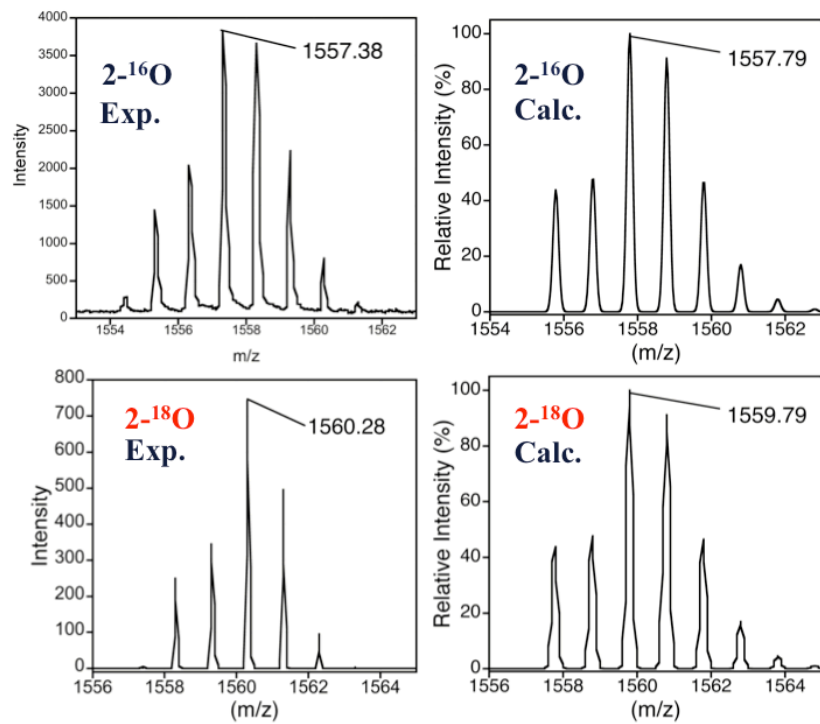


**Fig. S5.** Experimental and calculated LDI-TOF Mass spectra of **2-<sup>16</sup>O** and **2-<sup>18</sup>O**.

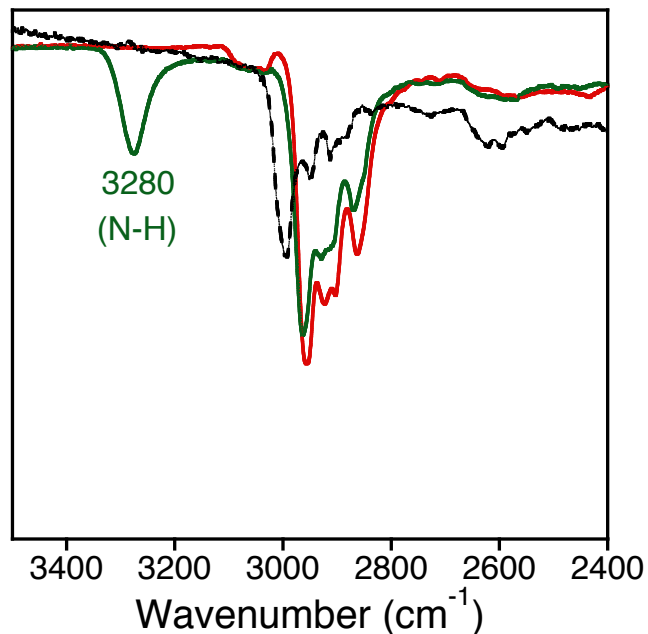


**Fig. S6.** ATR-IR spectra ( $2400 - 3500 \text{ cm}^{-1}$ ) of **2** (red line), **3-<sup>16</sup>O(BArF)** (green line), and **HBArF** (black dotted line).

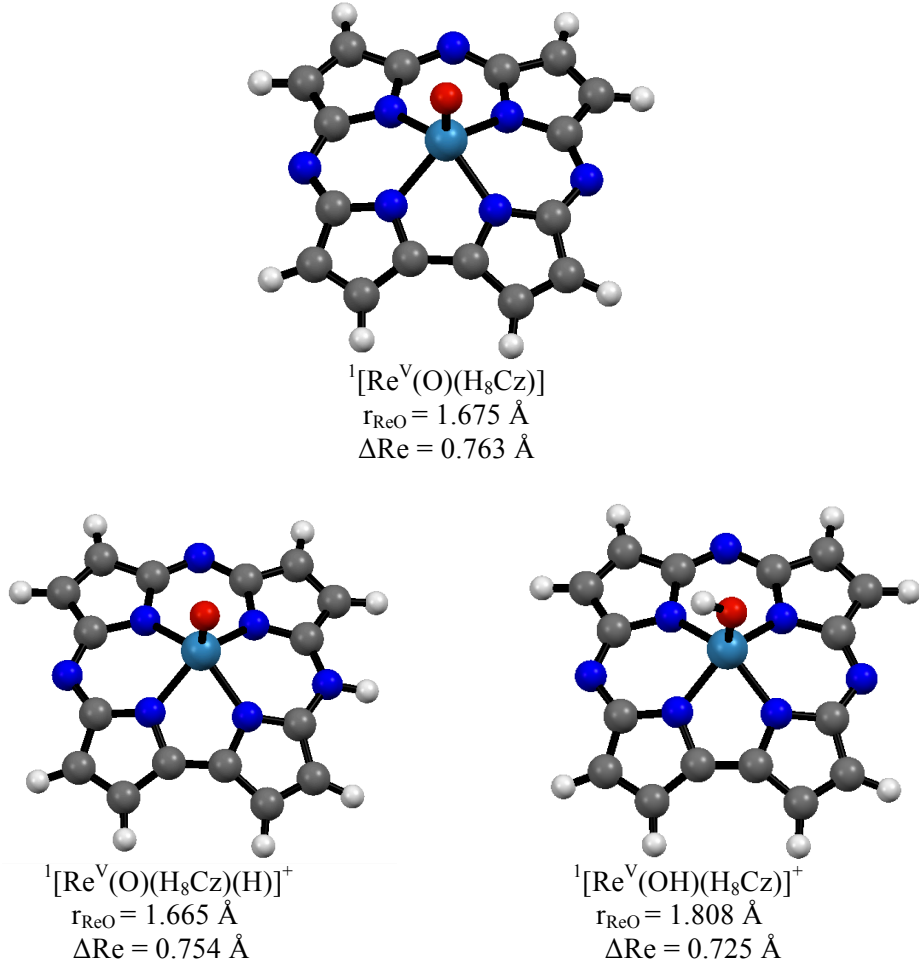


**Fig. S7.** Optimized geometries of  ${}^1[\text{Re}^{\text{V}}(\text{O})(\text{H}_8\text{Cz})]$  and its protonated states. Re-O bond distance ( $r_{\text{ReO}}$ ) and Re-Cz out-of-plane displacement (plane defined by the four internal nitrogens) ( $\Delta \text{Re}$ ) are shown in angstroms.

**Table S2.** Calculated absolute and relative energies of  ${}^1[\text{Re}^{\text{V}}(\text{OH})(\text{H}_8\text{Cz})]^+$  and  ${}^1[\text{Re}^{\text{V}}(\text{O})(\text{H}_8\text{Cz})(\text{H})]^+$ .

	$E^{\text{a}} (\text{Eh})$	$\Delta E (\text{kcal/mol})$
${}^1[\text{Re}^{\text{V}}(\text{OH})(\text{H}_8\text{Cz})]^+$	-1151.17539620	+29.06
${}^1[\text{Re}^{\text{V}}(\text{O})(\text{H}_8\text{Cz})(\text{H})]^+$	-1151.22171365	0.00

<sup>a</sup> Sum of electronic energy, zero-point energy, and thermal energy in atomic energy units.

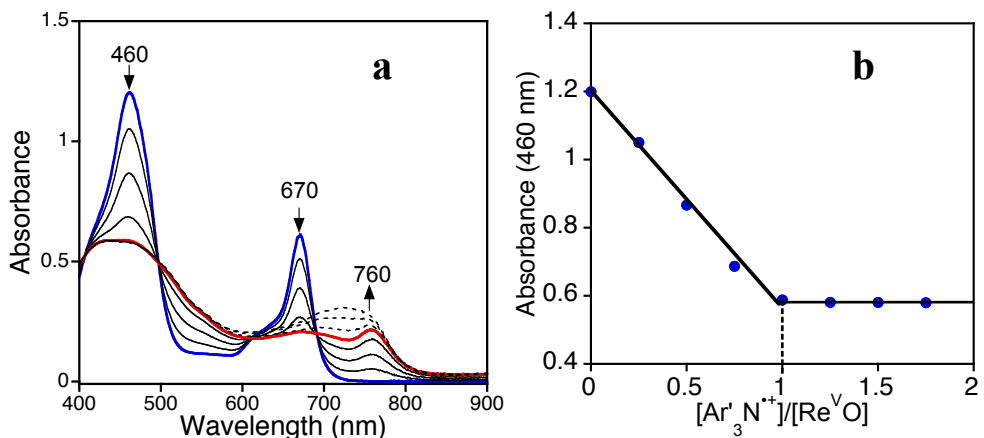


**Fig. S8.** a) UV-vis spectral changes of **2** observed upon addition of  $[\text{Ar'}_3\text{N}^{\bullet+}][\text{SbCl}_6^-]$  (0-1.75 equiv) in  $\text{CH}_2\text{Cl}_2$ . After complete formation of **4**( $\text{SbCl}_6^-$ ) at 1 equiv  $[\text{Ar'}_3\text{N}^{\bullet+}][\text{SbCl}_6^-]$  (red line), excess oxidant can be observed to grow in at  $\sim 730$  nm (black dotted lines). b) Spectral titration at 460 nm showing maximal formation of **4**( $\text{SbCl}_6^-$ ) at 1 equiv  $[\text{Ar'}_3\text{N}^{\bullet+}][\text{SbCl}_6^-]$ .

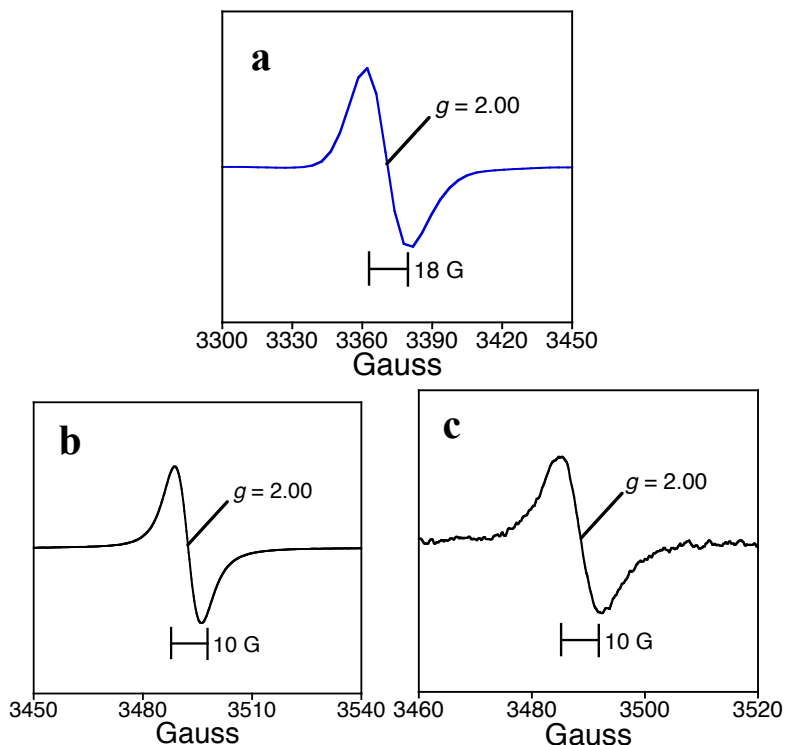


**Fig. S9.** X-band EPR spectra for **4** generated with a)  $[\text{Ar'}_3\text{N}^{\bullet+}][\text{SbCl}_6^-]$ , sample conc. = 1 mM, parameters:  $T = 16 \text{ K}$ , freq. = 9.427 GHz, power = 0.20 mW, mod. amp. = 10 G, mod. freq. = 100 kHz, receiver gain =  $5.02 \times 10^3$ . NS = 2. b)  $[\text{Ar'}_3\text{N}^{\bullet+}][\text{SbCl}_6^-]$ , sample conc. = 3 mM, parameters:  $T = 298 \text{ K}$ , freq. = 9.774 GHz, power = 0.20 mW, mod. amp. = 1 G, mod. freq. = 100 kHz, receiver gain =  $5.02 \times 10^4$ . NS = 4. Quantitation of the signal shows 94% yield of the oxidized product. c) CAN (1 equiv,  $\text{CH}_2\text{Cl}_2/\text{CH}_3\text{CN}$  4:1 v/v), sample conc. = 0.5 mM, parameters:  $T = 298 \text{ K}$ , freq. = 9.763 GHz, power = 0.20 mW, mod. amp. = 1 G, mod. freq. = 100 kHz, receiver gain =  $5.02 \times 10^4$ . NS = 4. Quantitation of the signal shows 87% yield of the oxidized product.

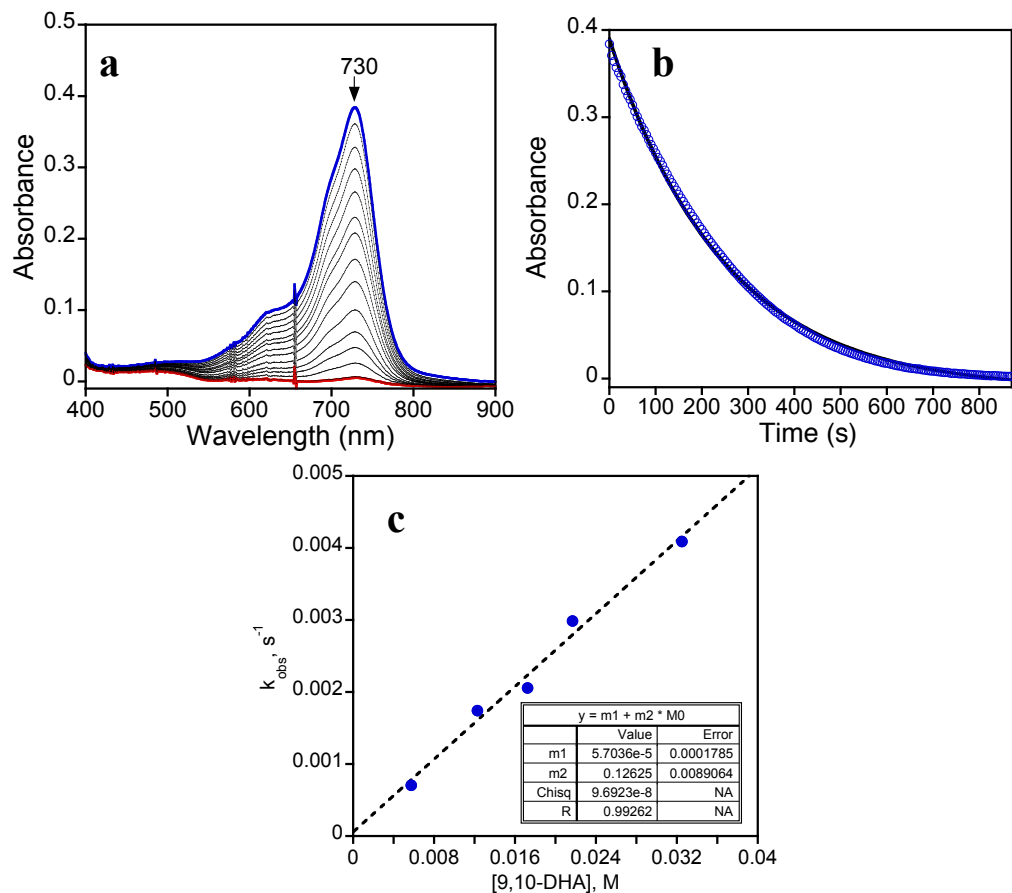
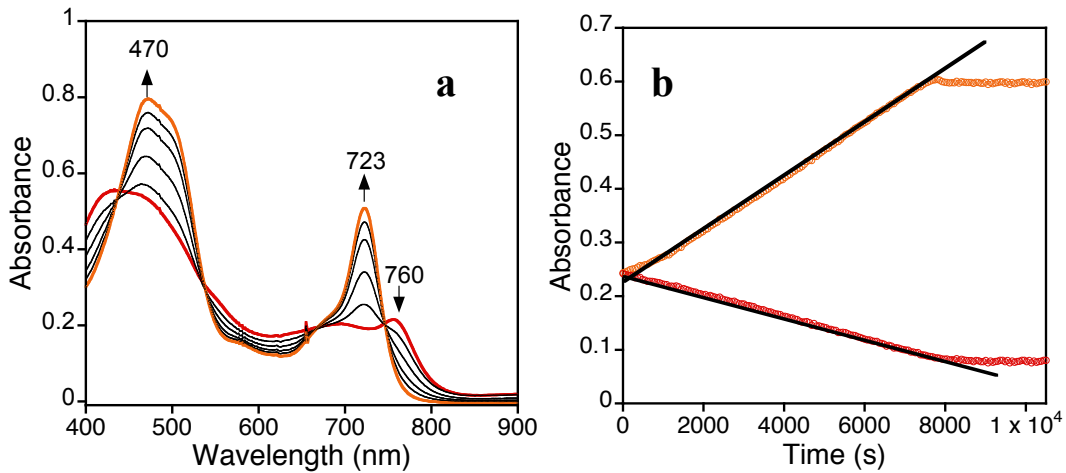


**Fig. S11.** a) Time-resolved UV-vis spectral changes for the reaction of  $[\text{Ar}'_3\text{N}]^+\text{SbCl}_6^-$  (12  $\mu$ M) and 9,10-DHA (0.033 M) in  $\text{CH}_2\text{Cl}_2$  at 25 °C. b) Changes in absorbance vs time for the decay of  $[\text{Ar}'_3\text{N}]^+\text{SbCl}_6^-$  (730 nm) (blue circles). c) Plot of  $k_{obs}$  versus [9,10-DHA].

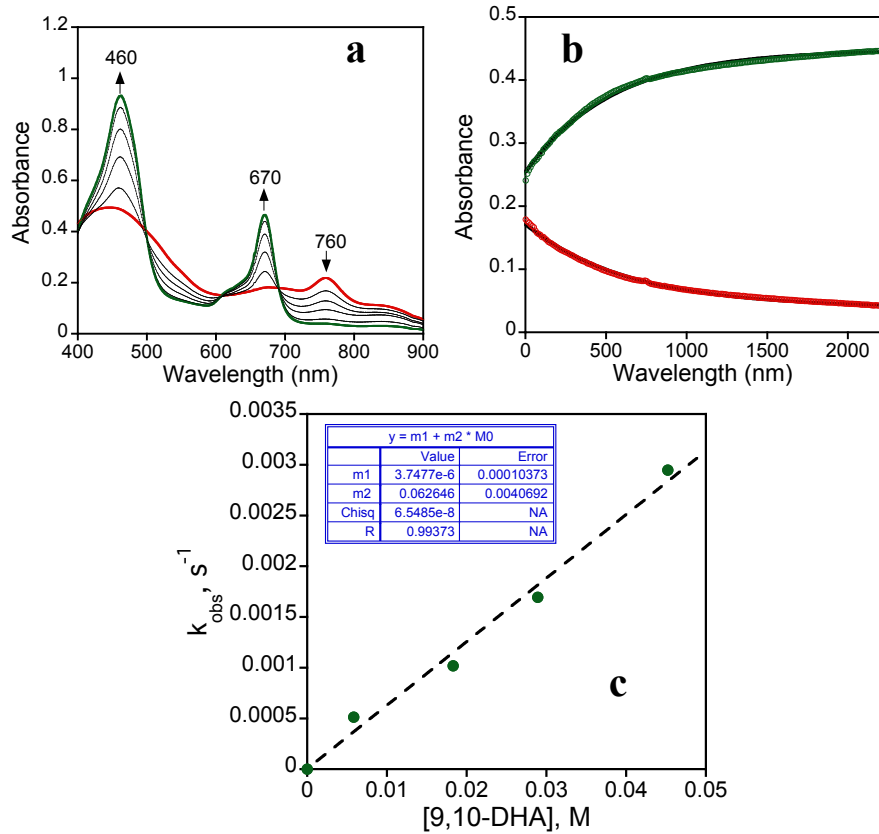


**Fig. S12.** a) Time-resolved UV-vis spectral changes for the reaction of **4** (12  $\mu\text{M}$ , generated with 1 equiv CAN) and 9,10-DHA (0.029 M) in  $\text{CH}_2\text{Cl}_2$  at 25  $^{\circ}\text{C}$ . b) Changes in absorbance vs time for the growth of **2** (670 nm) (green circles) and decay of **4** (760 nm) (red circles). c) Plot of  $k_{obs}$  versus [9,10-DHA]. Note the additional peak at 850 nm of **4**( $\text{NO}_3^-$ ) (red line), which does not appear in the spectrum of **4**( $\text{SbCl}_6^-$ ). This shoulder appears in the presence of the  $\text{NO}_3^-$  counterion (see Fig. S13).

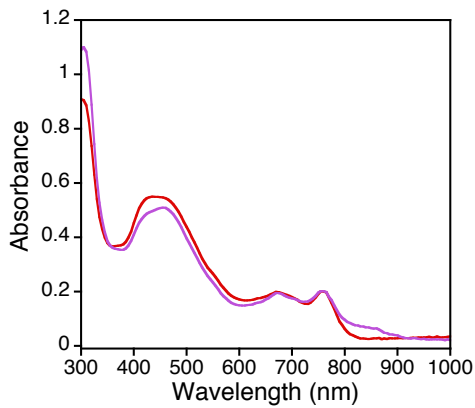


**Fig. S13.** UV-vis spectrum of **4**( $\text{SbCl}_6^-$ ) (12  $\mu\text{M}$ , 2 mL) before (red line) and after addition of  $[\text{Bu}_4\text{N}]^+[\text{NO}_3^-]$  (1 equiv, 20  $\mu\text{L}$  in  $\text{CH}_3\text{CN}$ ) (pink line) in  $\text{CH}_2\text{Cl}_2$  at 25  $^{\circ}\text{C}$ . A small excess of  $[\text{Ar}'_3\text{N}]^+[\text{SbCl}_6^-]$  was added to keep **4** oxidized. This UV-vis spectrum, with a shoulder at 850 nm, is similar to the spectrum of **4**( $\text{NO}_3^-$ ).

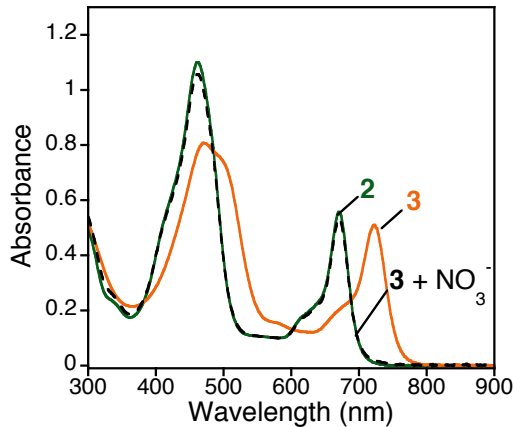


**Fig. S14.** UV-vis spectral change for the addition of  $[\text{Bu}_4\text{N}]^+[\text{NO}_3^-]$  (1 equiv) to **3(BArF)** ( $12 \mu\text{M}$ ) in  $\text{CH}_2\text{Cl}_2$  at  $25^\circ\text{C}$ . Complete deprotonation from **3** to **2** was observed.

### Calculated IR Spectra

Mode	${}^1[\text{Re}^{\text{V}}(\text{O})(\text{H}_8\text{Cz})]$		${}^1[\text{Re}^{\text{V}}(\text{O})(\text{H}_8\text{Cz})(\text{H})]^+$	
	Freq. (cm $^{-1}$ )	T $^2$	Freq. (cm $^{-1}$ )	T $^2$
6	80.05	0.095772	79.15	0.06585
7	89.38	1.510794	88.51	6.926334
8	113.51	0.465872	111.66	0.659254
9	138.3	0.118921	134.63	0.585434
10	147.47	0.2882	147.82	0.406581
11	205.1	0.542542	201.77	2.912995
12	206.2	1.664376	205.47	1.789809
13	225.32	0.286223	224.32	0.403143
14	253.5	4.604431	249.28	5.635323
15	274.28	0.262139	267.8	3.359652
16	274.98	1.886139	274.25	1.000199
17	286.01	0.732218	285.1	1.30586
18	307.09	0.097042	305.27	1.673359
19	314.84	5.317337	311.93	10.064328
20	349.75	0.236589	342.4	0.872675
21	365.4	0.735543	360.05	0.53348
22	400.69	3.740571	389.97	0.181579
23	420.94	7.586624	414.86	2.297054
24	451.31	16.849523	446.71	10.672032
25	462.4	3.178011	447.58	4.227642
26	467.57	0.000969	459.97	2.545775
27	472.7	0.419773	462.11	0.936467
28	483.57	1.444136	473.14	1.227062
29	491.93	0.092439	485.88	0.30499

30	507.66	0.029967	501.66	0.572417
31	565.85	4.065319	562.05	2.810338
32	650.54	2.61842	644.71	3.787776
33	676.37	0.008056	667.01	2.085782
34	684.23	2.83908	672.44	15.96326
35	698.71	0.157922	684.81	16.478614
36	719.34	0.054255	693.95	10.625203
37	720.26	14.124167	698.21	1.6768
38	742.26	7.716611	719.56	21.838687
39	744.15	0.999053	724.9	3.761173
40	747.7	6.805036	745.46	7.020386
41	751.29	10.594019	749.22	15.751984
42	796.03	4.647784	752.97	12.234103
43	797.55	6.361622	793.52	2.348397
44	804.5	60.868017	794.39	3.544724
45	807.66	0.426549	801.48	43.70226
46	809.17	12.53284	804.18	7.121092
47	815.59	3.725278	812.88	50.055345
48	827.92	2.185285	814.59	42.3782
49	829.02	88.786533	830.36	26.286079
50	894.49	1.813586	844.53	55.240693
51	921.58	0.24387	897.5	1.79782
52	922.71	0.481163	929.55	0.296097
53	942.66	0.544994	938.84	0.609174
54	943.38	0.281378	954.44	0.238128
55	1016.09	58.743285	964.58	0.498669
56	1046.35	0.338956	1014.19	151.128998
57	1054.38	107.56029	1044.77	47.458258
<b>58 (Re – O)</b>	<b>1055.41</b>	<b>38.569098</b>	<b>1063.76</b>	<b>14.649413</b>
59	1056.75	172.775156	1066.41	26.36627
60	1060.37	73.393451	1076.83	105.515643
61	1069.5	3.56609	1077.78	78.432912
62	1078.55	50.301921	1081.57	21.965748
63	1087.9	11.476246	1089.23	105.21035
64	1091.88	80.812824	1092.98	2.68881
65	1116.07	58.860075	1100.19	149.326064
66	1125.52	5.746333	1121.06	96.226669
67	1185.96	9.872383	1130.12	32.237811
68	1236.62	0.096101	1183.31	7.339567
69	1252.76	0.1416	1238.85	8.122288
70	1294.94	1.075519	1245.93	1.813538

71	1298.65	6.158835	1281.86	11.538007
72	1313.46	9.920753	1294.7	3.598219
73	1328.96	0.113058	1313.44	34.120467
74	1348.46	24.156775	1319.82	13.345041
75	1386.69	1.08304	1357.53	12.985568
76	1387.58	4.065021	1376.03	6.347972
77	1399.51	7.145669	1381.48	6.661297
78	1427.18	10.964555	1401.55	6.354065
79	1445.19	38.018789	1434.72	2.549565
80	1475.11	40.505992	1450.09	23.736881
81	1485.34	0.14446	1463.25	32.514305
82	1510	28.105762	1500.18	11.574134
83	1512.65	0.152126	1507.84	20.749529
84	1550.38	36.915969	1509.01	22.324185
85	1567.81	18.29368	1527.84	55.308676
86	1577.87	9.039576	1558.33	8.200797
87	1594.36	31.721016	1570.08	62.489605
88	1605.61	10.268146	1583.1	16.545012
89	1606.21	20.707365	1592.89	36.624719
90	1637.49	11.905938	1603.46	7.561346
91	3280.38	0.105942	1633.64	49.671173
92	3281.15	1.022485	1661.07	48.067678
93	3285.5	0.083144	3282.62	1.901151
94	3285.79	0.024121	3287.42	2.648929
95	3298.64	0.191771	3289.32	1.837572
96	3300.63	0.188142	3292.33	3.126089
97	3302.78	0.209838	3300.83	8.661823
98	3303.75	0.127456	3304.37	9.444241
99			3307.12	9.561835
100			3307.4	5.92429
<b>101 (N-H)</b>			<b>3638.66</b>	<b>226.789741</b>

### Cartesian Coordinates of Optimized Geometries reported:

<sup>1</sup>[Re<sup>V</sup>(O)(H<sub>8</sub>Cz)]:

```

Re 0.11277999485348 -0.04354651995799 0.00525687123730
O 1.62217153135538 0.48389451596239 0.50433590159918
N -1.22881261970766 -0.05846179156661 1.46079482974050
C -1.50747062270434 -1.00616597399044 2.40886956760102
C -2.45064230000190 -0.42241219236571 3.31101087316002
C -2.78185991849741 0.83372745594364 2.83491733498032
C -2.03128668608238 1.05089744267390 1.64969163762837
C -1.97152880940419 1.92212443338929 0.54405556020284
C -2.63037541513638 3.05955638149910 0.00782059301587
C -2.20196811418575 3.20901003203484 -1.29926547437078
C -1.28947045169663 2.14815989552504 -1.59275696235777
N -1.12532175561899 1.43673158806972 -0.43461050601355

```

N	-0.78321348322363	1.79768615567891	-2.77200058750220
C	-0.19050144703526	0.62363717900428	-2.93154539503809
C	0.20839155898782	0.07910852870779	-4.19861715382477
C	0.61790628159333	-1.20937686336094	-3.99829275685699
C	0.48657202599050	-1.49818490407828	-2.60023282658181
N	0.04223561169303	-0.35139246762993	-1.96444889475949
N	0.68830842158160	-2.68330616448655	-2.04406076045320
C	0.38556536164685	-2.93427414044697	-0.77935719566477
C	0.40594948708567	-4.23067693255646	-0.16761514420243
C	-0.08409716335492	-4.10123958502560	1.10149739306594
C	-0.42389001684113	-2.72197294835290	1.31101169109077
N	-0.07500811917018	-2.02411936406373	0.15715566449496
N	-1.06470833352210	-2.26027227355130	2.37469345343195
H	-0.25477410658817	-4.87381643153892	1.83857411054163
H	0.72791604963558	-5.12805098495126	-0.67704819995051
H	0.95211039124008	-1.93120522115839	-4.73039662095854
H	0.13037539218361	0.62277634111606	-5.13003876479664
H	-2.52401846610731	3.95363233365460	-2.01407826940796
H	-3.36199857673381	3.66837572178654	0.52158160761431
H	-3.50654728073248	1.51552454320935	3.25926102530475
H	-2.85639183150231	-0.92291147917347	4.17904418802977

<sup>1</sup>[Re<sup>V</sup>(O)(H<sub>8</sub>Cz)(H)]<sup>+</sup>:

Re	-0.05486232385350	-0.03273419970397	-0.00079491294361
O	1.44803007326705	0.48781667087240	0.49225369135695
N	-1.39967852413623	-0.02971103054905	1.46845031410893
C	-1.70396463715122	-0.93527215262634	2.41722653673632
C	-2.65349576343897	-0.37325335265193	3.31181699225047
C	-2.9688015233475	0.88326461397684	2.81904622757701
C	-2.20541527469875	1.09098533393686	1.64184845178451
C	-2.13200470409407	1.94685971999313	0.53336827772622
C	-2.78445159379401	3.09644734518181	-0.00724889528301
C	-2.34949758030642	3.24149324745004	-1.30388776563658
C	-1.43612794497716	2.16551526446964	-1.59576044659507
N	-1.27862876222187	1.45485392212498	-0.43716935472384
N	-0.93554798592931	1.81704835517555	-2.76808434746164
C	-0.33983808812292	0.63985507002360	-2.93419285745523
C	0.04815592248450	0.10245504974106	-4.20739417454275
C	0.45749667588559	-1.18712113821623	-4.01351702137829
C	0.33375546230868	-1.47780034916184	-2.61492548042993
N	-0.10392117882052	-0.32929726147343	-1.96930219762283
N	0.52900430974499	-2.66069514536016	-2.06185484353944
C	0.23191005527409	-2.93155661489518	-0.80327116805173
C	0.26297120781159	-4.22284980340622	-0.19637072395832
C	-0.23000228560979	-4.10576301943360	1.08180513900609
C	-0.56374682162169	-2.73810588342962	1.26185965653418
N	-0.24602320753011	-2.02388864366619	0.14196406977819
N	-1.20277400969516	-2.19431723678130	2.33312525800182
H	-1.41723696076379	-2.82922172964326	3.09210249481973
H	-0.38087706779035	-4.89498458029029	1.80649940235711
H	0.59354645643555	-5.12096843250539	-0.69905382700129
H	0.78592242871471	-1.90674476700260	-4.75068364121807
H	-0.03444791148503	0.64974070666796	-5.13630193114927
H	-2.65788692329119	3.98955601275016	-2.02161775053621
H	-3.51003687147697	3.71247165923616	0.50617210475822
H	-3.69497854997826	1.56700196267146	3.23749383726110
H	-3.07798331880470	-0.85436858347507	4.18239196547023

<sup>1</sup>[Re<sup>V</sup>(OH)(H<sub>8</sub>Cz)]<sup>+</sup>:

Re	-0.10468566153686	-0.03492401351044	-0.05135216230077
N	-0.14785705167621	-0.33890092317065	-1.98623921944053
C	-0.39374656877499	0.63431968952422	-2.97650472022052
N	-0.99820779717532	1.79686001498593	-2.81719258120062
C	-1.49423926907399	2.14531090719763	-1.64435450818398
C	-2.37875221619388	3.21599388704387	-1.33285310039092
C	-2.78641205541957	3.08313134190193	-0.01640153873684
C	-2.14606038470243	1.94204291849405	0.51919465247143

N	-1.29613990902286	1.43436327644356	-0.46982711382015
C	-2.20326186027007	1.07791290268837	1.61315374947058
N	-1.40512796814878	-0.04483844177515	1.40018504499200
C	-1.69517451074069	-0.99762628517047	2.35822270227180
C	-2.60624330232876	-0.39588765341608	3.27641627178343
C	-2.92611106211449	0.86665506749658	2.81329289916957
H	-3.62422382374392	1.56133933179542	3.26052716939985
H	-2.98752239809212	-0.88722793734265	4.16090627723224
N	-1.25230237501291	-2.24128883382792	2.33119023470351
C	-0.60443576774376	-2.69926826970290	1.27521253002845
C	-0.23583829227333	-4.06530744807421	1.07695248265945
C	0.24281342183519	-4.20015920923377	-0.19722916435056
C	0.19350075358776	-2.91996364322542	-0.82635107598003
N	0.49020883054477	-2.67536364806040	-2.08589335361551
C	0.28841655202575	-1.49698480640089	-2.64069859943746
C	0.42649825946325	-1.19921109206111	-4.02763420746310
C	0.01679457970317	0.09168433411751	-4.23011651993663
H	-0.05187313633023	0.63576945960134	-5.16214631195783
H	0.77420638791751	-1.91589199675262	-4.75887369638238
N	-0.26792063685423	-1.98975575126241	0.10950453310464
H	0.58821492376966	-5.09548412165595	-0.69527181132378
H	-0.37928816334954	-4.83167984577484	1.82633143252119
H	-3.49499472836766	3.71220176797616	0.50526246772410
H	-2.69046441187854	3.97028517949568	-2.04247776172900
O	1.52578838749411	0.50458464032849	0.51415185690645
H	2.13912028448398	1.19436691132710	0.22505523203194